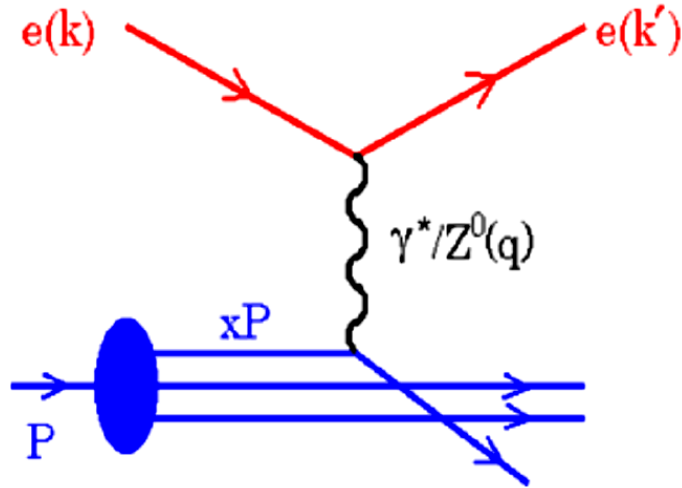


PDF decomposition at low x

S. Glazov, DESY,
Paris December 2010

Prologue: ep as a proton structure probe

Neutral current Deep Inelastic Scattering (DIS) cross section:



$$\frac{d^2\sigma^\pm}{dx dQ^2} = \frac{2\pi\alpha^2 Y_+}{Q^4 x} \sigma_r^\pm =$$

$$= \frac{2\pi\alpha^2 Y_+}{Q^4 x} \left[F_2(x, Q^2) - \frac{y^2}{Y_+} F_L(x, Q^2) \mp \frac{Y_-}{Y_+} x F_3 \right]$$

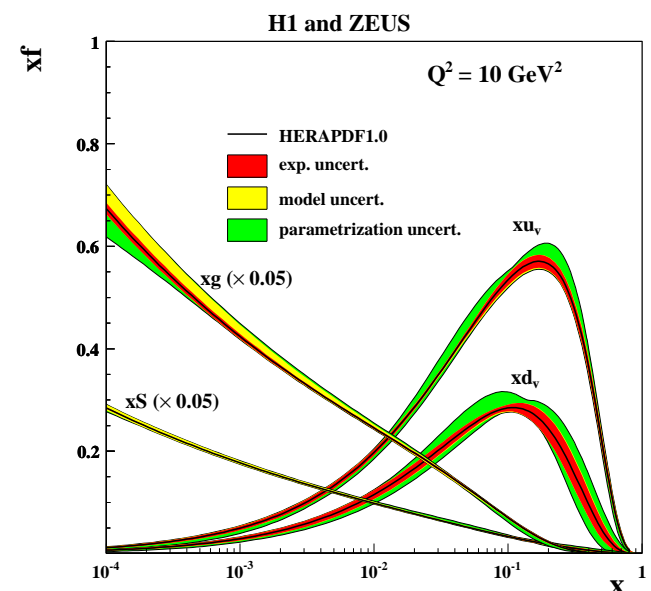
where factors $Y_\pm = 1 \pm (1 - y)^2$ and y^2 define polarisation of the exchanged boson and $y = Q^2/(Sx)$.

Kinematics is determined by boson virtuality Q^2 and Bjorken x .

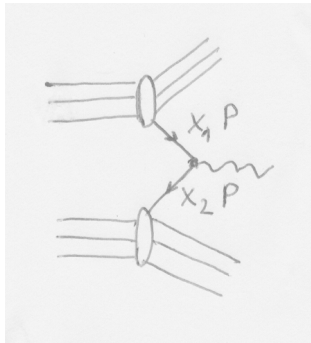
At leading order:

$$\begin{aligned} F_2 &= x \sum e_q^2 (q(x) + \bar{q}(x)) \\ xF_3 &= x \sum 2e_q a_q (q(x) - \bar{q}(x)) \\ \sigma_{CC}^+ &\sim x(\bar{u} + \bar{c}) + x(1 - y)^2(d + s) \\ \sigma_{CC}^- &\sim x(u + c) + x(1 - y)^2(\bar{d} + \bar{s}) \end{aligned}$$

$xg(x)$ — from F_2 scaling violation, jets and F_L



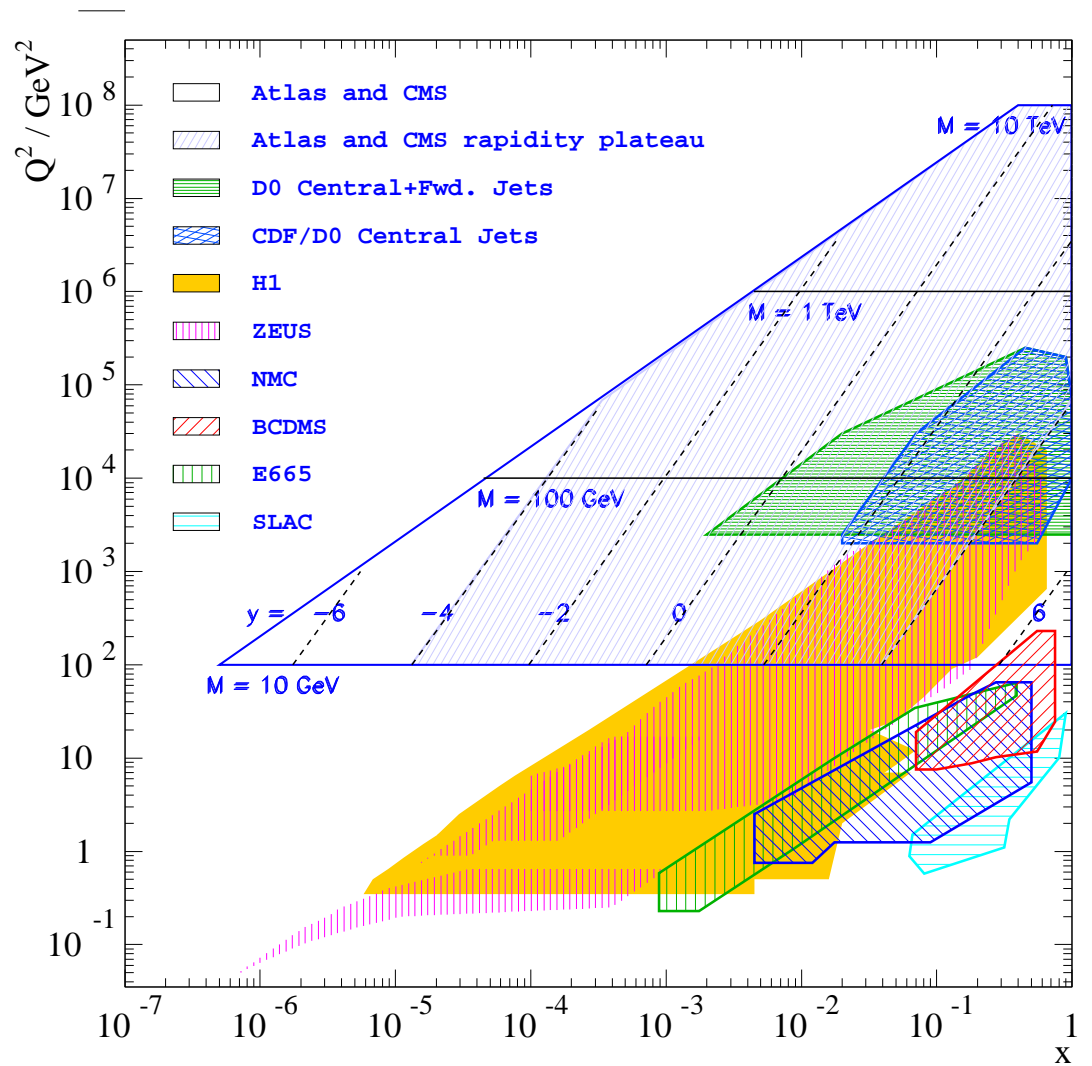
HERA and LHC kinematics



x_1, x_2 are momentum fractions.

Factorization theorem states that cross section can be calculated using universal partons \times short distance calculable partonic reaction.

$$x_{1,2} = \frac{M}{\sqrt{S}} \exp(\pm y)$$



Neutral Current Processes at the LHC

Double differential cross section:

$$\frac{d\sigma^2}{dMdy} = \frac{4\pi\alpha^2(M)}{9} \cdot M \cdot P(M) \cdot \Phi(y, M^2).$$

Propogator for γ exchange:

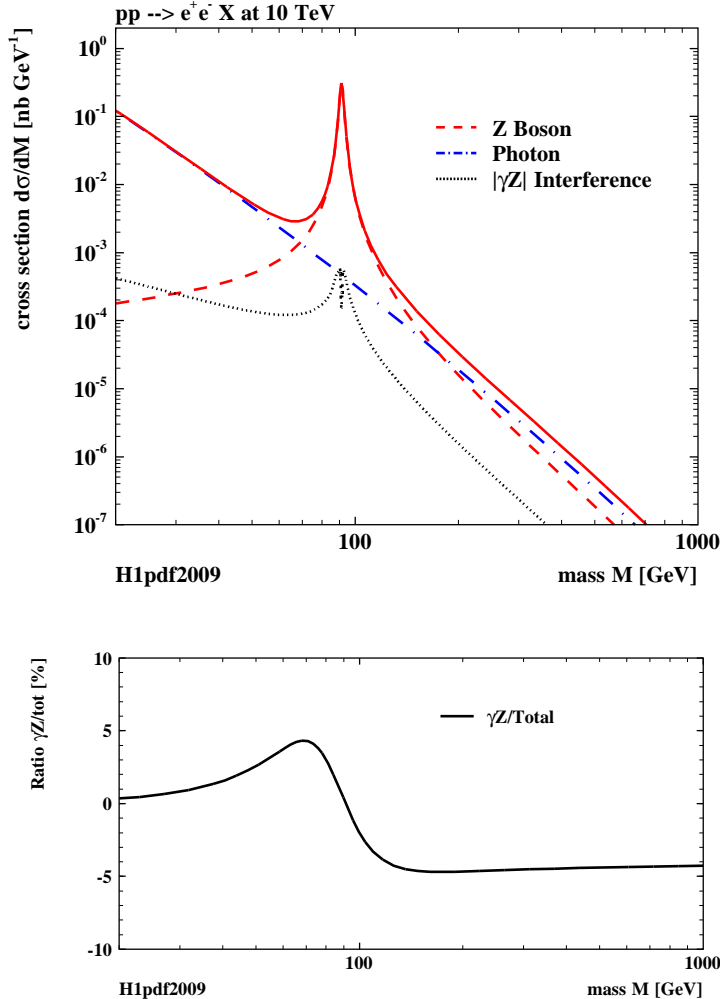
$$P_\gamma(M) = \frac{1}{M^4},$$

pure Z exchange:

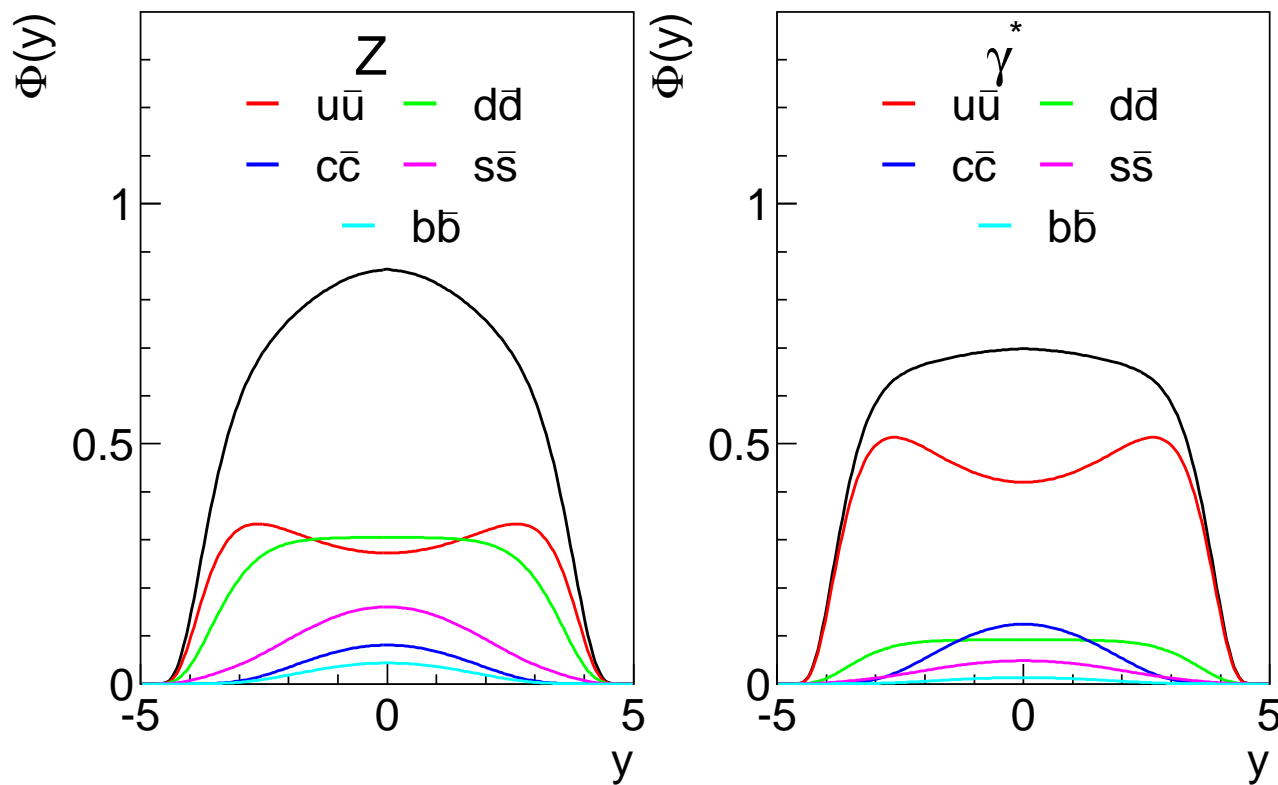
$$P_Z(M) = \frac{k_Z^2(v_e^2 + a_e^2)}{(M^2 - M_Z^2)^2 + \Gamma_Z^2 M_Z^2},$$

where $k_Z = (4 \sin^2 \theta_W \cos^2 \theta_W)^{-1}$, and
 γZ interference:

$$P_{\gamma Z}(M) = \frac{k_Z v_e (M^2 - M_Z^2)}{M^2 \left[(M^2 - M_Z^2)^2 + \Gamma_Z^2 M_Z^2 \right]},$$



Z and low mass DY production flavour decomposition



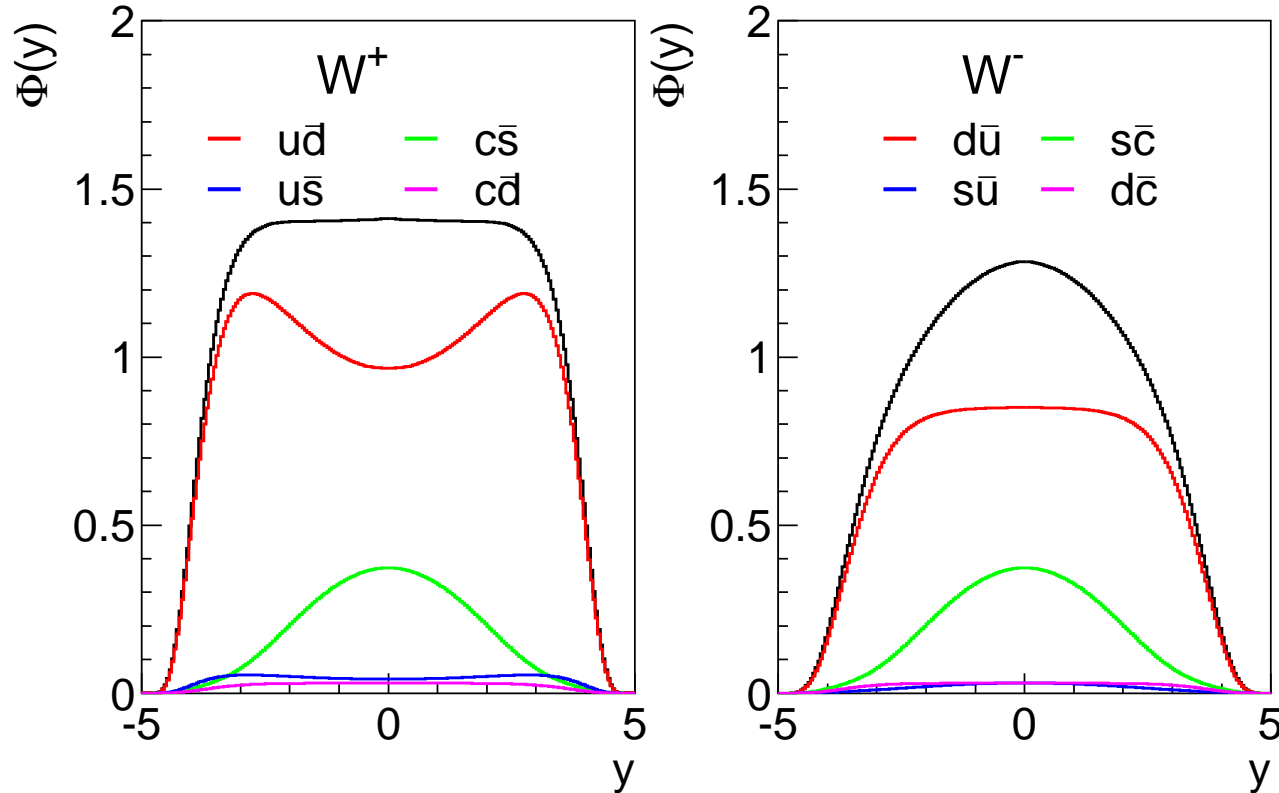
Z vs γ^* are sensitive to U/D ratio:

$$Z \sim 0.29(u\bar{u} + c\bar{c}) + 0.37(d\bar{d} + s\bar{s} + b\bar{b})$$

$$\gamma^* \sim 0.44(u\bar{u} + c\bar{c}) + 0.11(d\bar{d} + s\bar{s} + b\bar{b})$$

Contribution from $\gamma - Z$ interference is small.

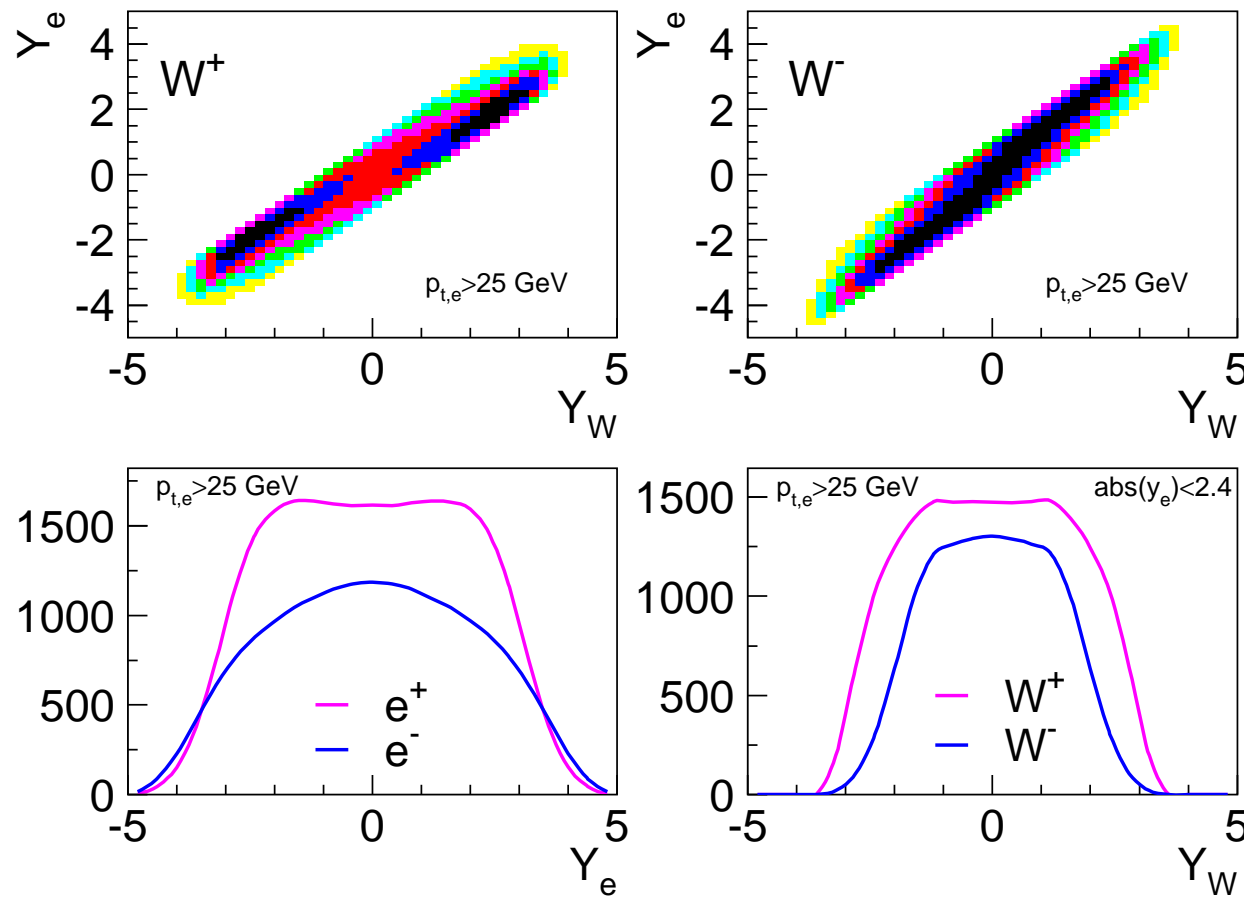
W^+ and W^- production flavour decomposition



W^+ (W^-) production is sensitive to $u\bar{d}$ ($d\bar{u}$) as well as $c\bar{s}$ ($s\bar{c}$) flavour combinations and to lesser extend to Cabibbo suppressed pairs:

$$W^+ \quad \sim 0.95(u\bar{d} + c\bar{s}) + 0.05(u\bar{s} + c\bar{d})$$
$$W^- \quad \sim 0.95(d\bar{u} + s\bar{c}) + 0.05(d\bar{c} + s\bar{u})$$

W decays



For W^\pm production the observables are lepton p_t and η . V-A structure of the decay modifies rapidity distribution of the lepton vs the boson. W^+ production accesses higher y for a given η_e range.

(plots based on LO MCFM, HERAPDF1.0)

NNLO Predictions for W, Z production cross sections

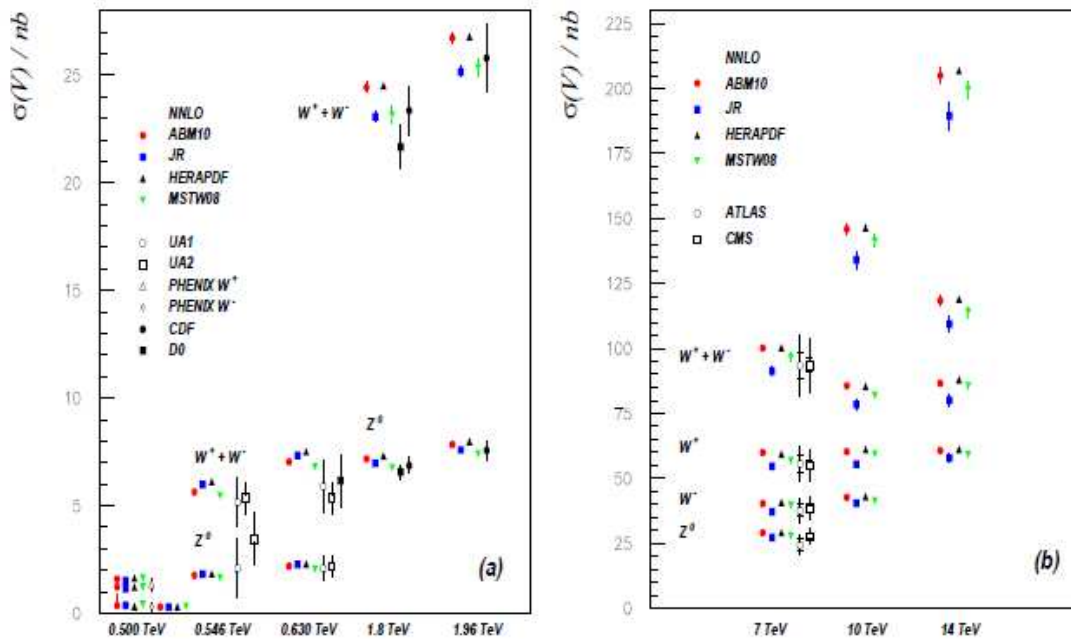
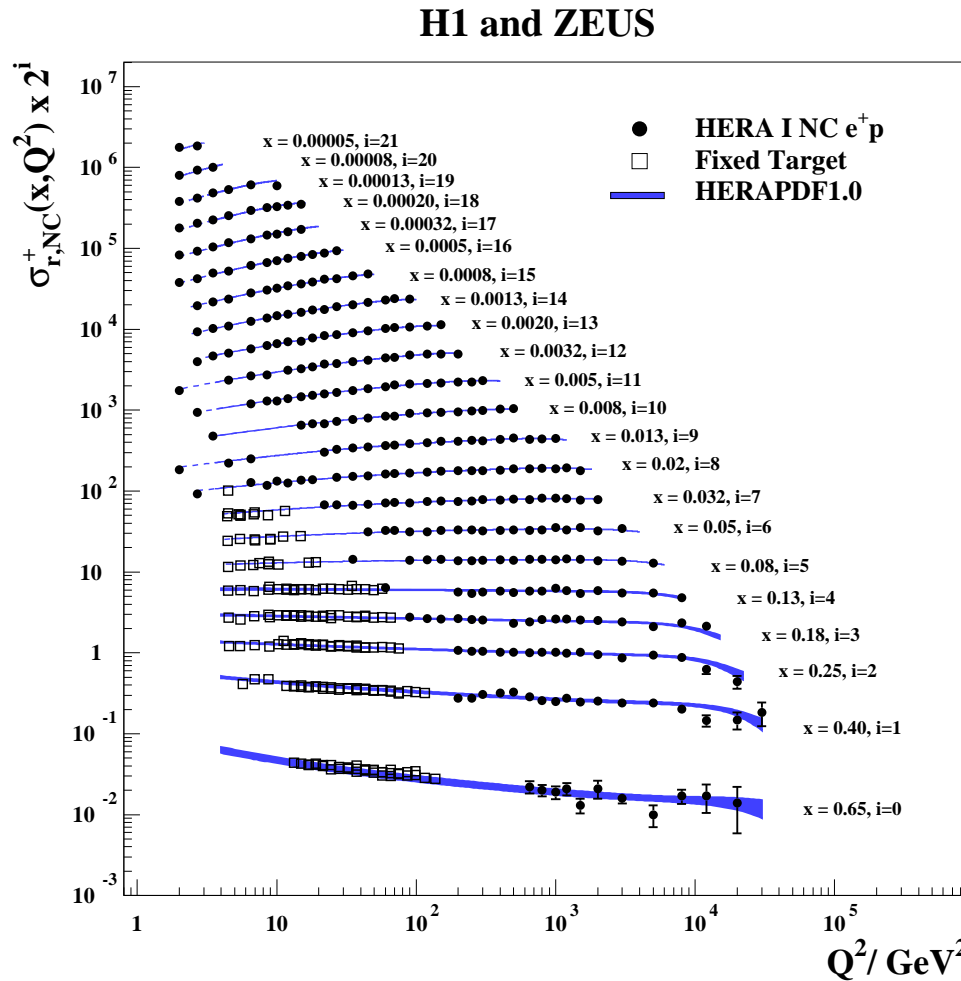


Figure 1: Comparison of different NNLO predictions for the inclusive W^+ , W^- , W^\pm , and Z^0 boson production cross sections in $p\bar{p}$ annihilation and pp scattering ($\sqrt{S} = 0.5$ TeV) based on the pdfs of recent NNLO analyses, ABM, ABKM, JR, HERAPDF, MSTW08, MSTW10, and the corresponding experimental data by UA1, UA2, PHENIX, CDF, CDF1, D0, ATLAS, CMS. Left panel (a): the lower energy region corresponds to $p\bar{p}$ collisions, except at 0.5 TeV, which refers to pp scattering. For the latter case the predictions refer to (from above) $W^+ + W^-$, W^+ , W^- and the ones for Z^0 are given to the right of the ones for W^- . Right panel (b): LHC energies (pp collisions); the inner error bars refer to $(\sigma_{\text{stat}}^2 + \sigma_{\text{syst}}^2)^{1/2}$ and the total error is obtained by adding the luminosity error in quadrature.

Recent analysis based on existing NNLO PDF sets.

S. Alekhin *et. al.*, arXiv:1011.6259.

Combined HERA data



HERA data precision is similar to fixed target experiments. Good consistency between H1 and ZEUS. Stringent test of DGLAP evolution.

Combination of the published H1/ZEUS data collected at HERA-I for CC,NC, $e^\pm p$ mode. 14 publications, 1402 input and 741 output σ_r measurements, 110 correlated experimental error sources. For NC $e^+ p$, $6 \cdot 10^{-7} < x < 0.65$ and $0.045 < Q^2 < 30000 \text{ GeV}^2$.

Combination:

$$\chi^2/dof = 637/656$$

QCD Fit (to the combined HERA data with $Q^2 \geq 3.5 \text{ GeV}^2$):

$$\chi^2/dof = 574/582$$

HERAPDF1.0 Fit Settings

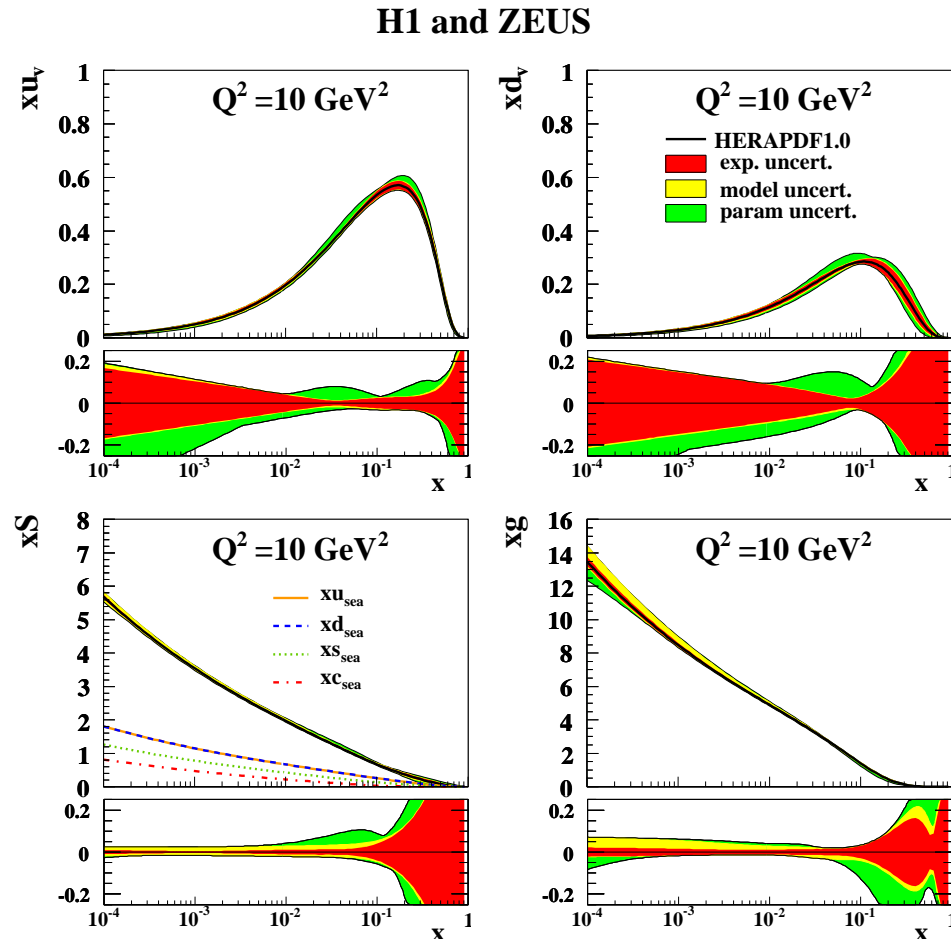
- Input: combined HERA-I data for $e^\pm p$ NC and CC scattering. Well understood experimental errors and minimal theoretical uncertainties: pure ep data far from low W region, no jets.
- (N)NLO evolution, RT-VFNS for charm and bottom, $\alpha_S = 0.1176$.
- Evolution starting scale $Q^2 = 1.9 \text{ GeV}^2$, below $m_c^{\text{model}} = 1.4 \text{ GeV}$. Start fitting data at $Q_{\min}^2 = 3.5 \text{ GeV}^2$.
- Fitted PDFs are xg , xu_v , $xd_v(x)$, $x\bar{U}$, $x\bar{D}$ where $x\bar{U} = x\bar{u}$ and $x\bar{D} = x\bar{d} + x\bar{s}$ at the starting scale. For the strange, $x\bar{s} = f_s x\bar{D}$ with $f_s = 0.31$ is assumed.
- Standard parameterisation form

$$xf(x) = Ax^B(1 - x)^C(1 + \epsilon\sqrt{x} + Dx + Ex^2)$$

with only significant ϵ , D and E terms kept.

- A_g , A_{u_v} , A_{d_v} fixed by sum rules. Extra constraints for small x behaviour of d and u -type quarks: $B_{u_v} = B_{d_v}$, $B_{\bar{U}} = B_{\bar{D}}$, $A_{\bar{U}} = A_{\bar{D}}(1 - f_s)$

QCD analysis of the HERA combined data



HERAPDF1.0 — NLO
QCD analysis of the
combined HERA data.

Separation of **experimental**,
model and **parameterisation**
uncertainties.

Accurate xS and xg at low x
due to precise measurement
of F_2 .

Large uncertainties for va-
lence quarks at low x .

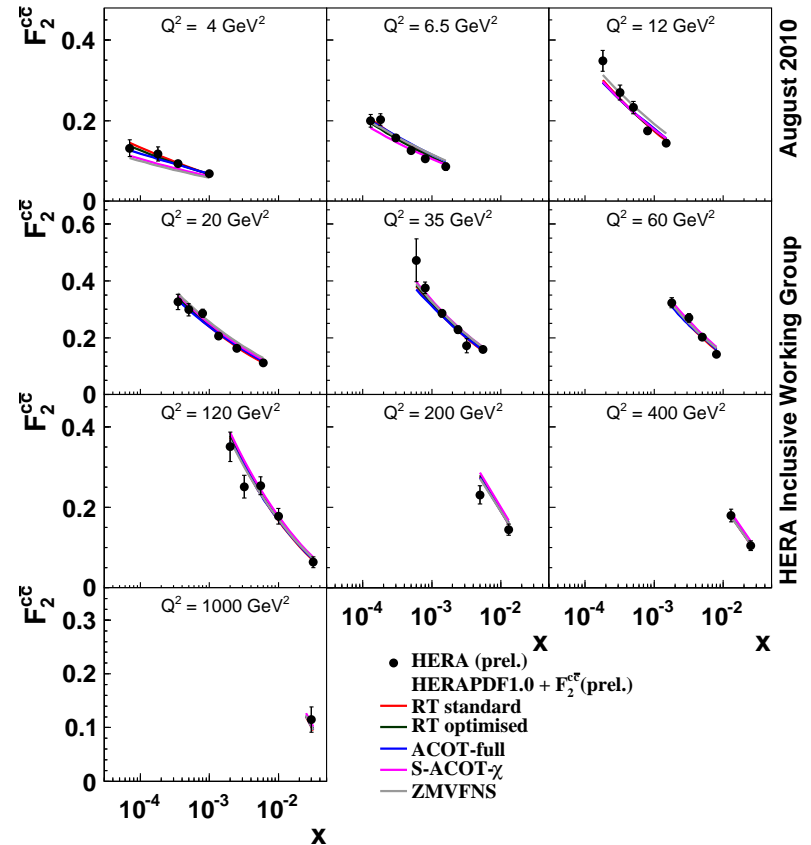
Decomposing u and c densities at low x

Inclusive structure function F_2 is sensitive to

$$F_2 \sim 4(U + \bar{U}) + (D + \bar{D}),$$

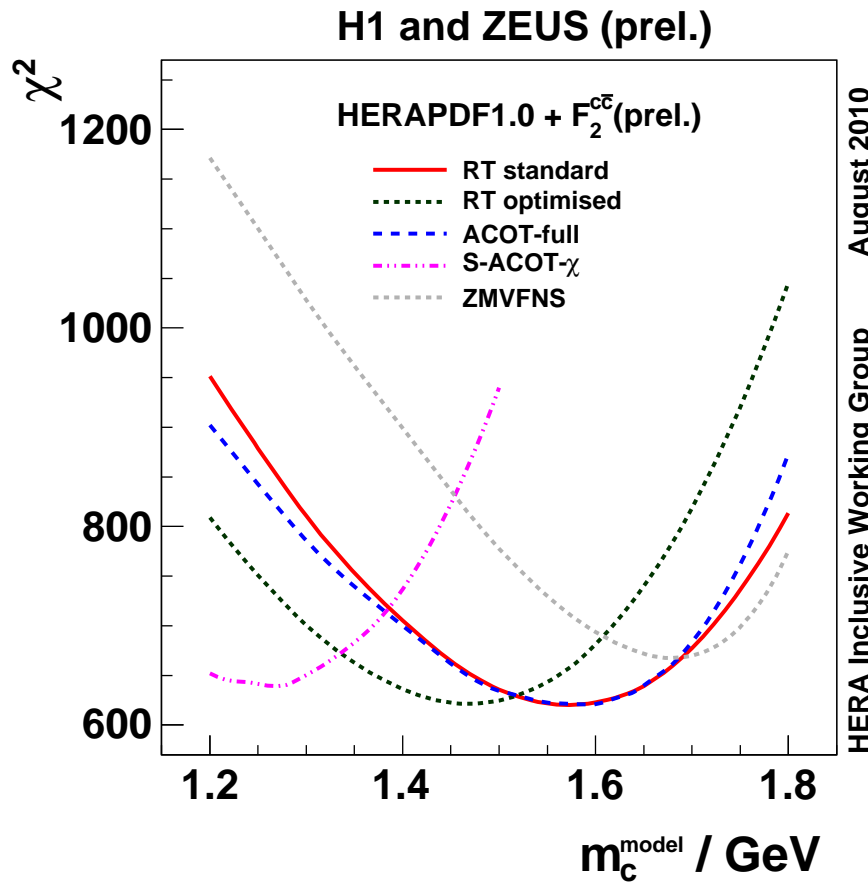
where $U = u + c$ and $D = d + s + b$. At low x , contribution of charm to F_2 reaches 30%.

Determination of charm contribution is a mixed theoretical/experimental problem: it can be calculated given the gluon density, however description of the charm threshold is complicated leading to a number of matching schemes (RT, ACOT, FNOLL...).



Combined HERA F_2^{cc} data reaches 5 – 10% precision per point, can be used to study different HF models.

Scan of m_c^{model}

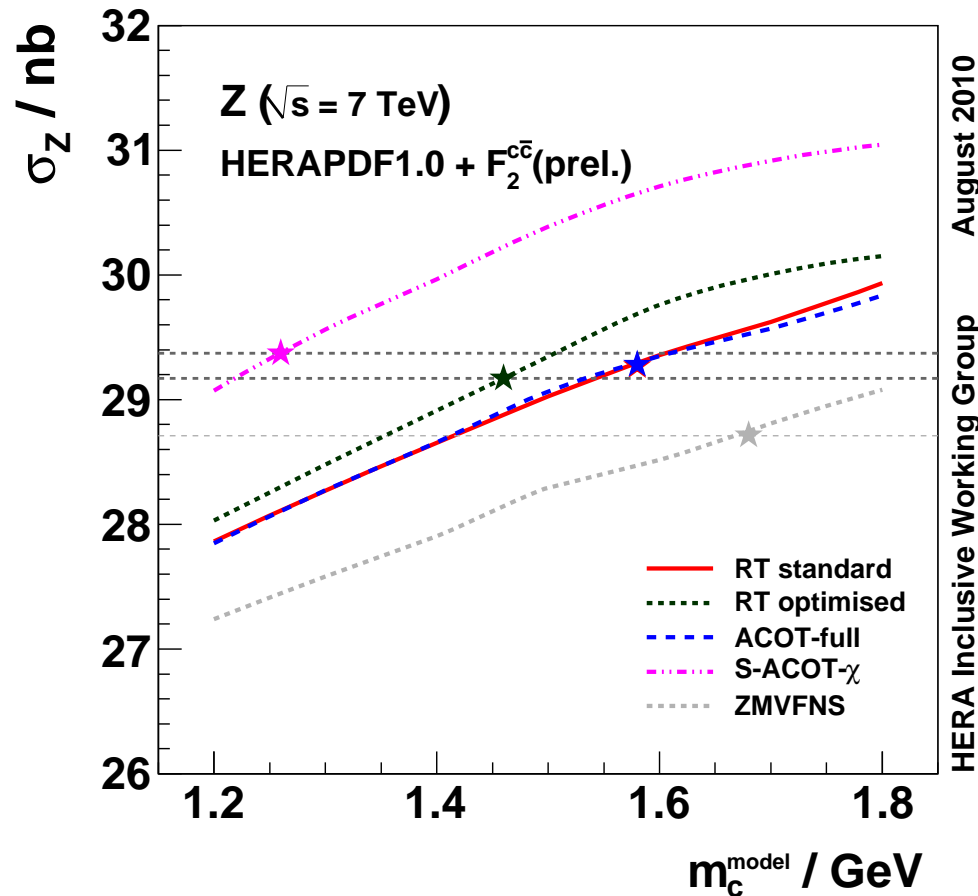


Fits to combined HERA inclusive and $F_2^{c\bar{c}}$ data using different models for HF treatment.

All models use a parameter m_c^{model} which is related to the charm pole mass. Use it as a free parameter to tune the models to the charm data.

→ depending on the model, large spread of the values, but similar χ^2 values at $m_c^{\text{model}}(opt)$ (except ZMVFN).

Sensitivity of LHC predictions to the charm

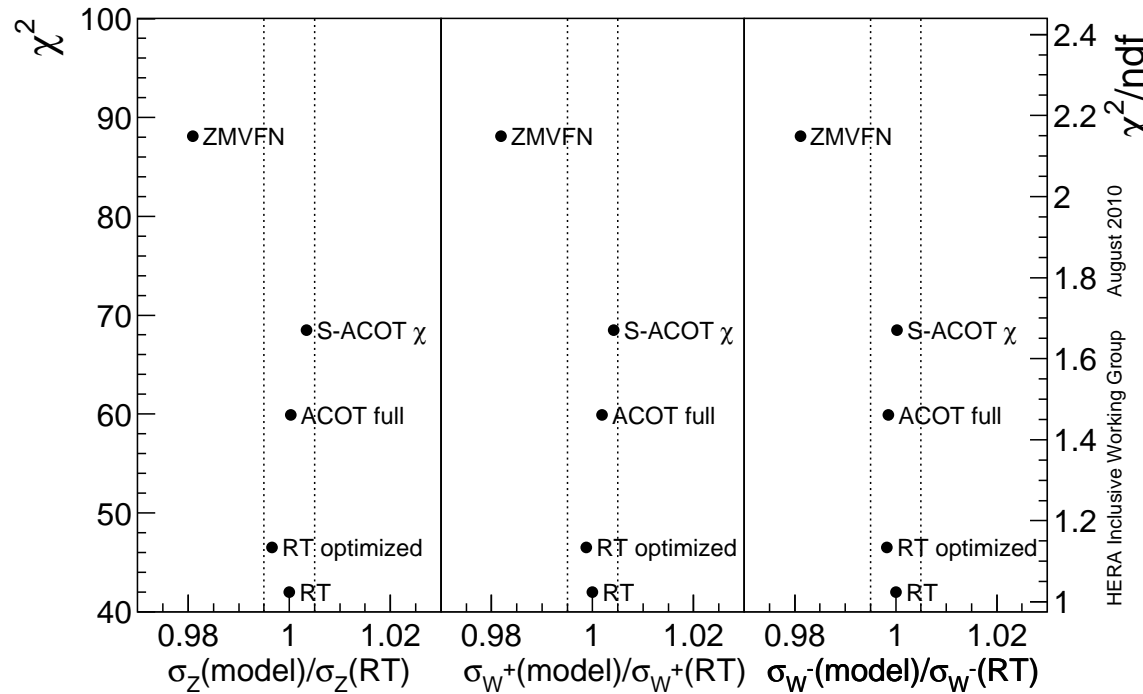


Large $\sim 7\%$ spread of the total cross section prediction for m_c^{model} scan between $1.2 - 1.8 \text{ GeV}$ and also for a fixed m_c^{model} when considering different models. However, the spread is reduced to $< 0.5\%$ (excluding ZMVFNS) when predictions are evaluated at the $m_c^{\text{model}}(opt)$ values.

More info including table of predictions, uncertainties can be found at

http://www.desy.de/h1zeus/combined_results/heavy_flavours/MCScan/charmfit.pdf

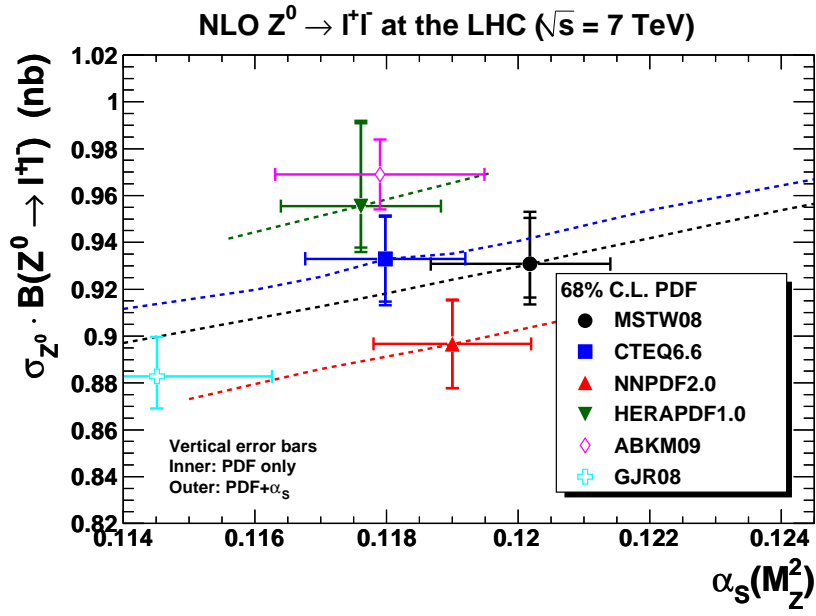
LHC predictions vs charm data fit



- F_2^{cc} data excludes simplified model of ZMVFN.
- Models with smaller χ^2/ndf return smaller spread in predictions, all within 0.5%.

→ HERA F_2^{cc} data and upcoming full NNLO calculations should provide $c-u$ decomposition with (probably) sufficient accuracy for the LHC.

Importance of c -density: Z-at the LHC



Large spread of predictions can be to large extend explained by different charm treatment.

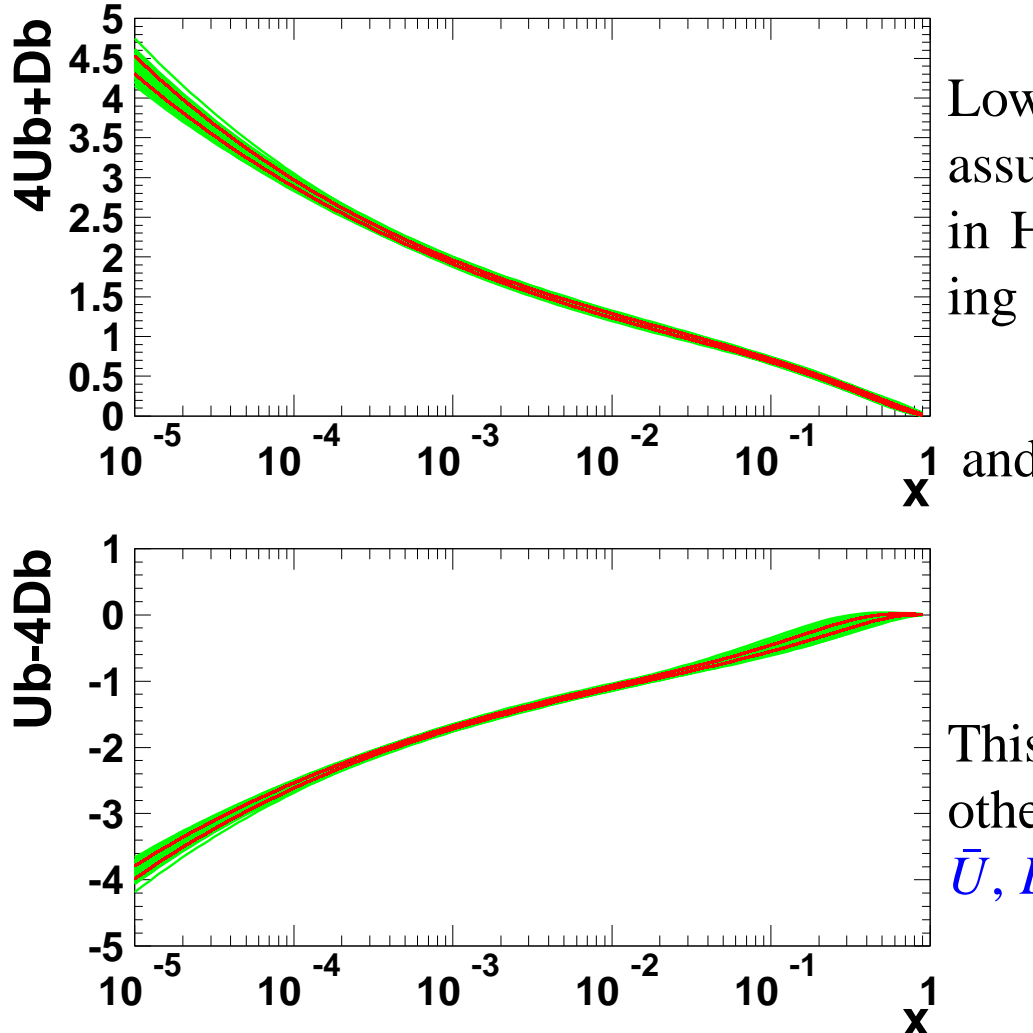
- CTEQ6.5: S-ACOT- χ with $m_C^{\text{model}} = 1.3 \text{ GeV}$ (close to optimal 1.26 GeV)
- MSTW08: RT with $m_C^{\text{model}} = 1.4 \text{ GeV}$ (optimal is 1.58 GeV)
- NNPDF2.0: ZMVFNS with $m_C^{\text{model}} = \sqrt{2} = 1.41 \text{ GeV}$ (optimal is 1.68 GeV).

Recently MSTW08 released sets with different values of m_C^{model} .

Comparing CTEQ6.6 and MSTW08 for the same values of α_S and m_C^{model} close to optimal values, one finds (MCFM4.7, PDF4LHC benchmark settings):

$$\sigma_Z \times \text{Br}(Z^0 \rightarrow \ell\ell) = \begin{cases} 0.949 \text{ nb} (\text{MSTW08}, \alpha_S = 0.118, m_C^{\text{model}} = 1.6 \text{ GeV}) \\ 0.947 \text{ nb} (\text{CTEQ6.6}, \alpha_S = 0.118, m_C^{\text{model}} = 1.3 \text{ GeV}) \end{cases}$$

Decomposition of U and D



Low x behaviour of d and u is assumed to be the same. Forced in HERAPDF1.0 fit by requiring

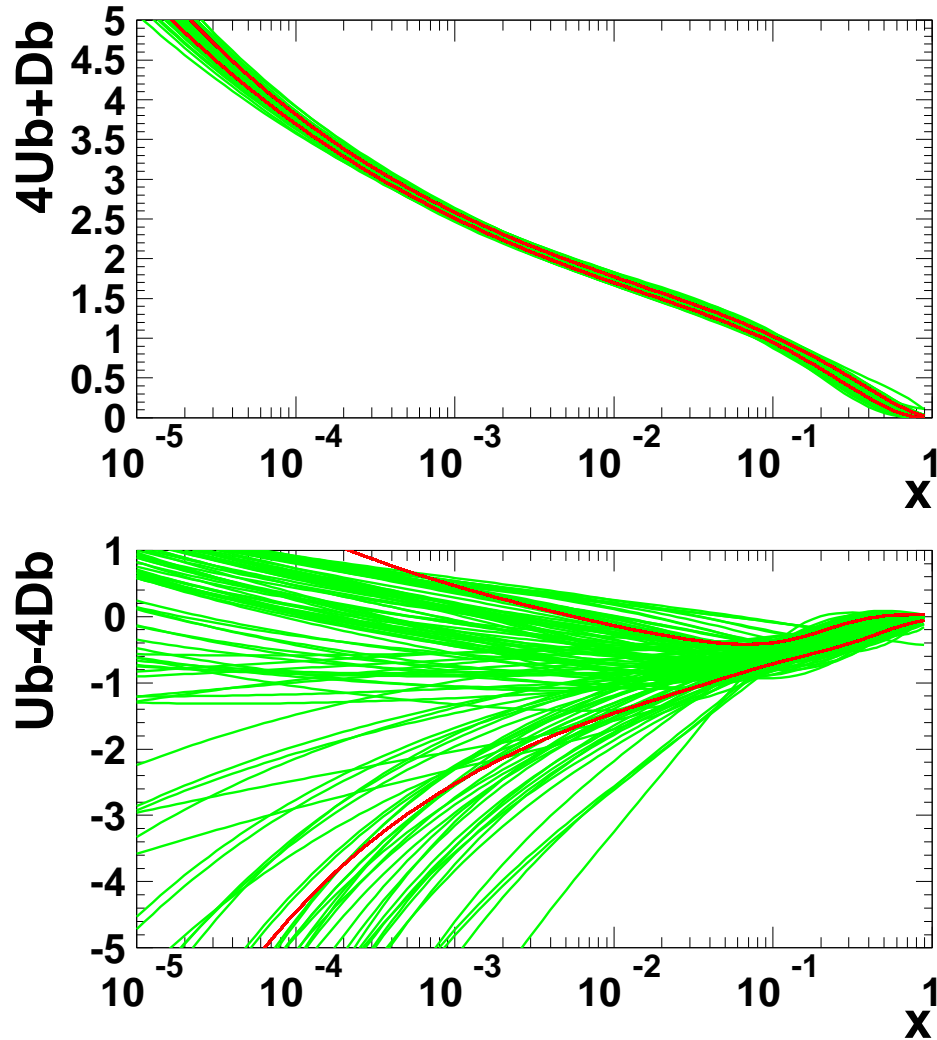
$$B_{\bar{U}} = B_{\bar{D}}$$

$$A_{\bar{U}} = A_{\bar{D}}(1 - f_s)$$

This imposes constraint on other linear combinations of \bar{U}, \bar{D} vs $4\bar{U} + \bar{D}$.

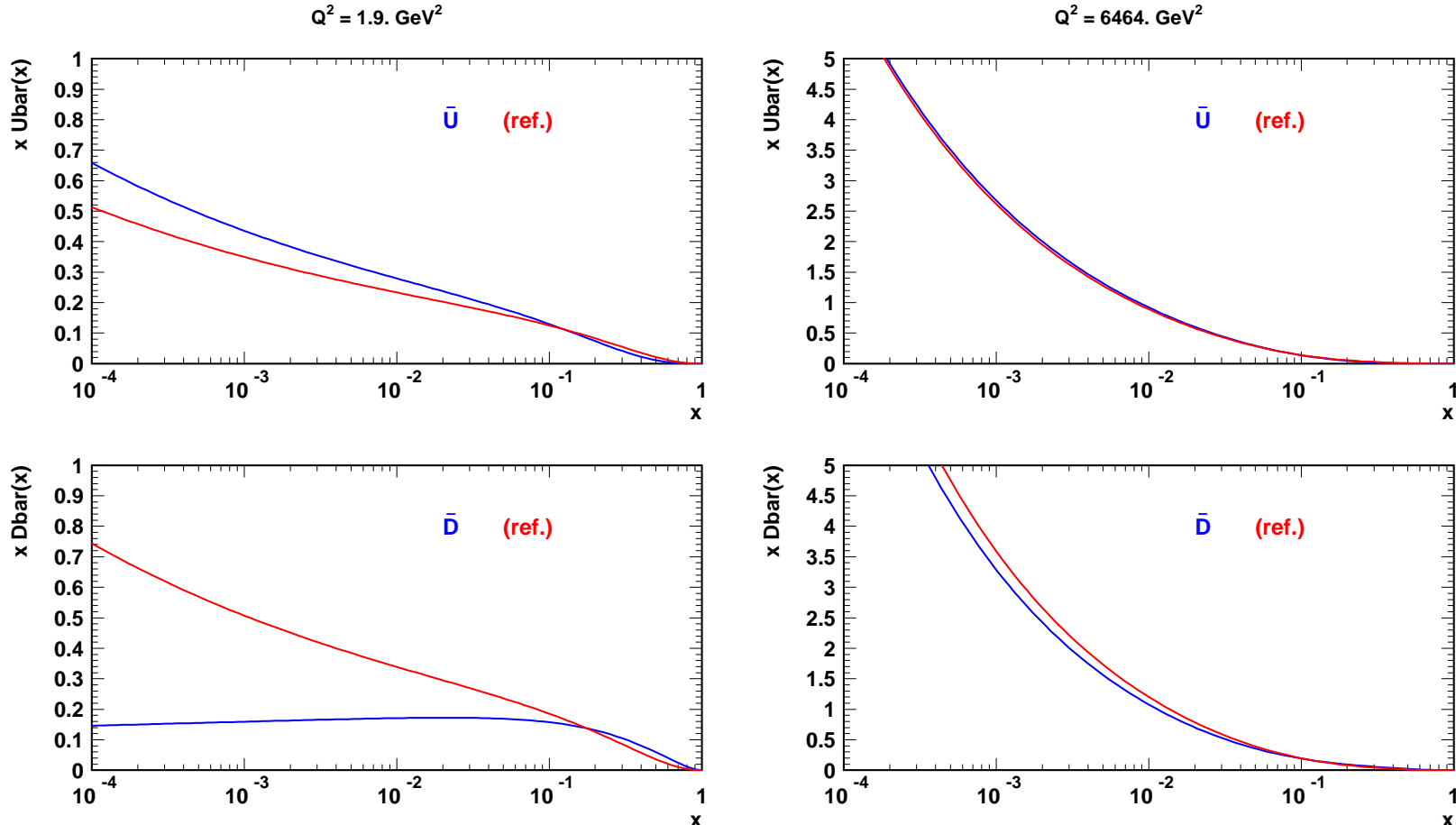
Uncertainties are determined MC method, green lines: individual replicas, red: RMS.

HERA fits without $d = u$ assumption



Unconstrained fit preserves narrow $4\bar{U} + \bar{D}$ but orthogonal combination $\bar{U} - 4\bar{D}$ has very large spread. The only significant constraint comes from the positivity of the PDFs, $\bar{D} > 0, \bar{U} > 0$, which is built in the parameterisation.

\bar{U} and \bar{D} densities in the unconstrained fit

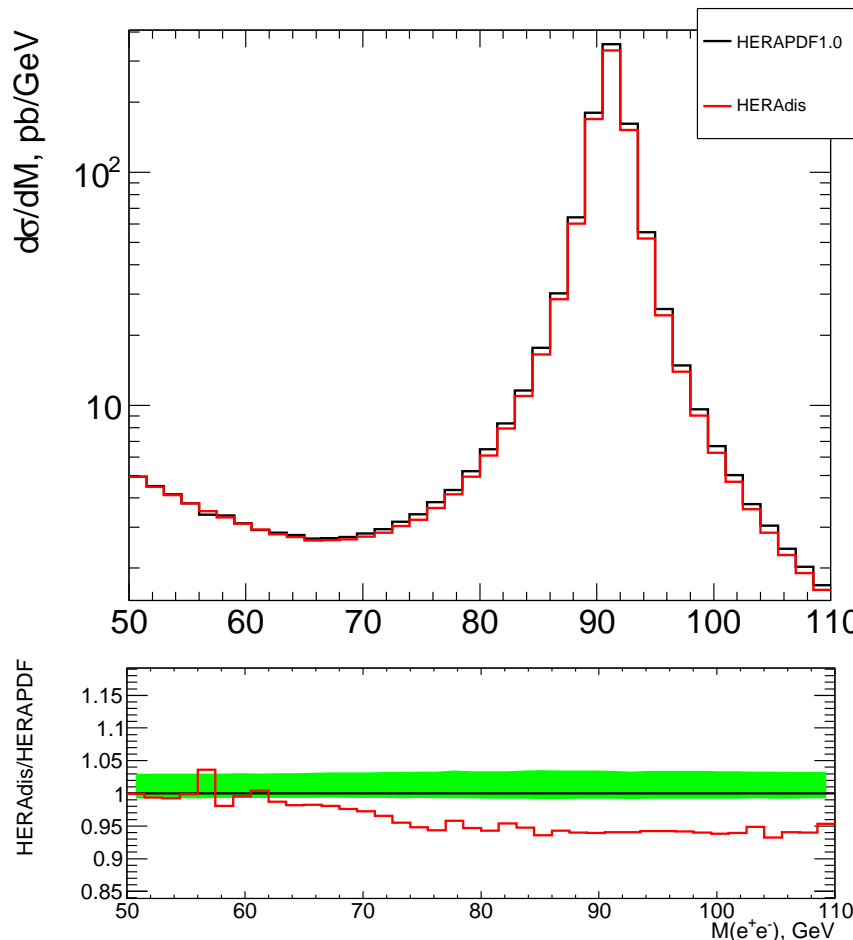


Central unconstrained fit prefers solution with low \bar{D} and increased \bar{U} . The difference is dramatic at the starting scale, but it remains sizable at the M_W scale too.

LHAPDF grid file for the unconstrained fit:

https://www.desy.de/h1zeus/combined_results/proton_structure/Fits/HERAPDF1.0u.LHgrid.gz

Low mass DY vs Z for U over D decomposition

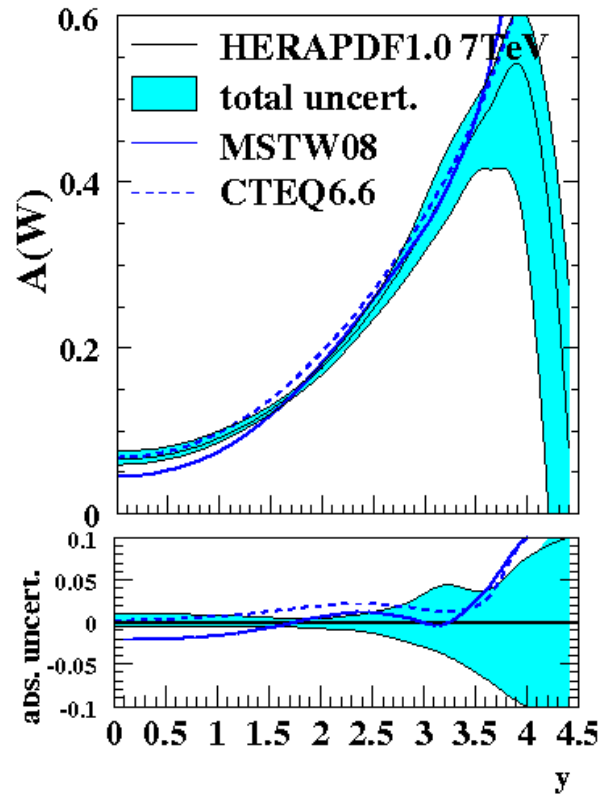
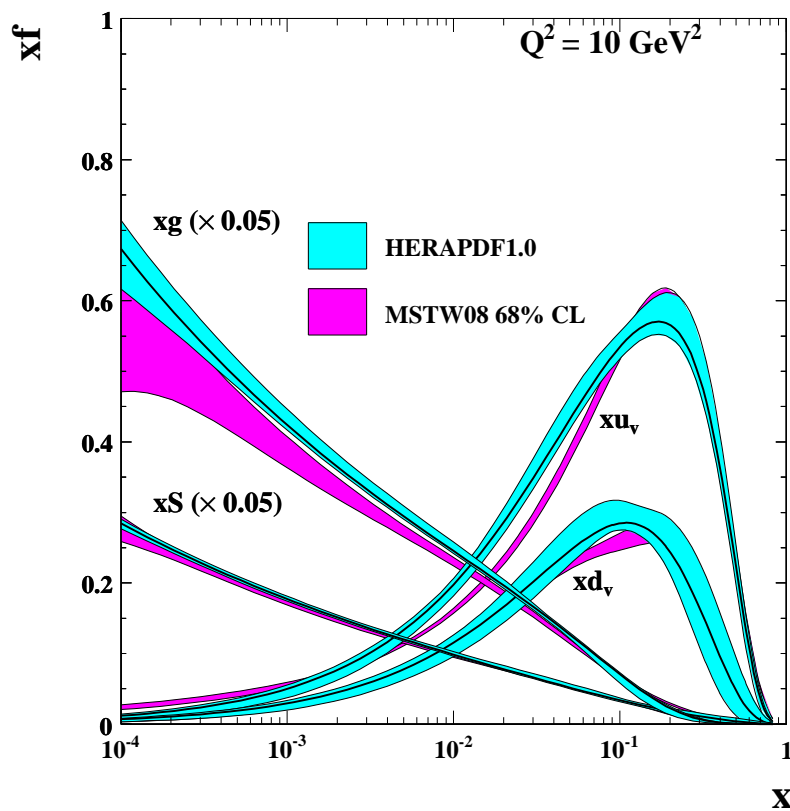


Since γ^* exchange has the same sensitivity to the quark flavours as the measurement of F_2 at HERA, unconstrained fit agrees with HERAPDF1.0 at low $M_{e^+e^-}$, but sizable lower at $M_{e^+e^-} = M_Z$.

based on NLO MCFM

To separate \bar{U} and \bar{D} for the same (Q^2, x) region a good observable is the ratio of $d\sigma/dy$ for Z production at $\sqrt{s} = 7$ TeV and DY for $M_{e^+e^-} = M_Z/2$ at $\sqrt{s} = 14$ TeV at the LHC.

Valence quarks at low x



Significant differences between valence quark densities from different PDF groups. Assuming $\bar{u} \approx \bar{d}$, W^\pm asymmetry is given by

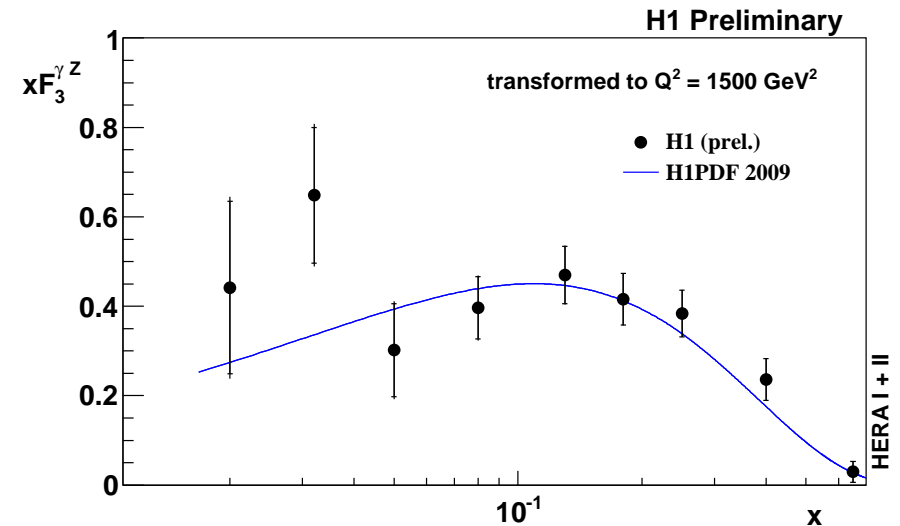
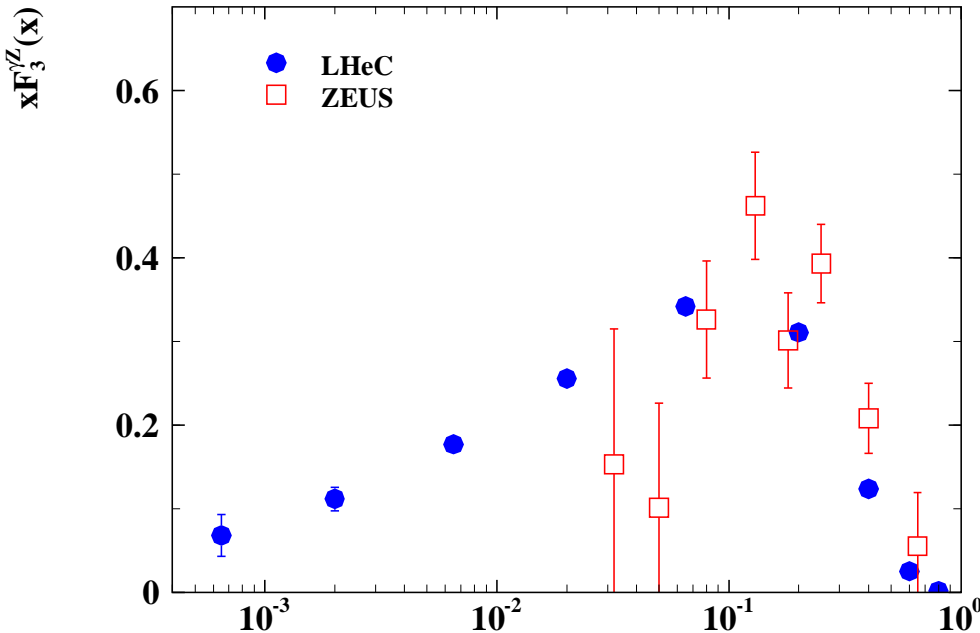
$$A \approx \frac{u_v - d_v}{u + d}$$

Discrepancy at $x = 0.01$ corresponds to $y_W = 0$ for $s = 7 \text{ TeV}$.

Valence quarks: existing sources of information

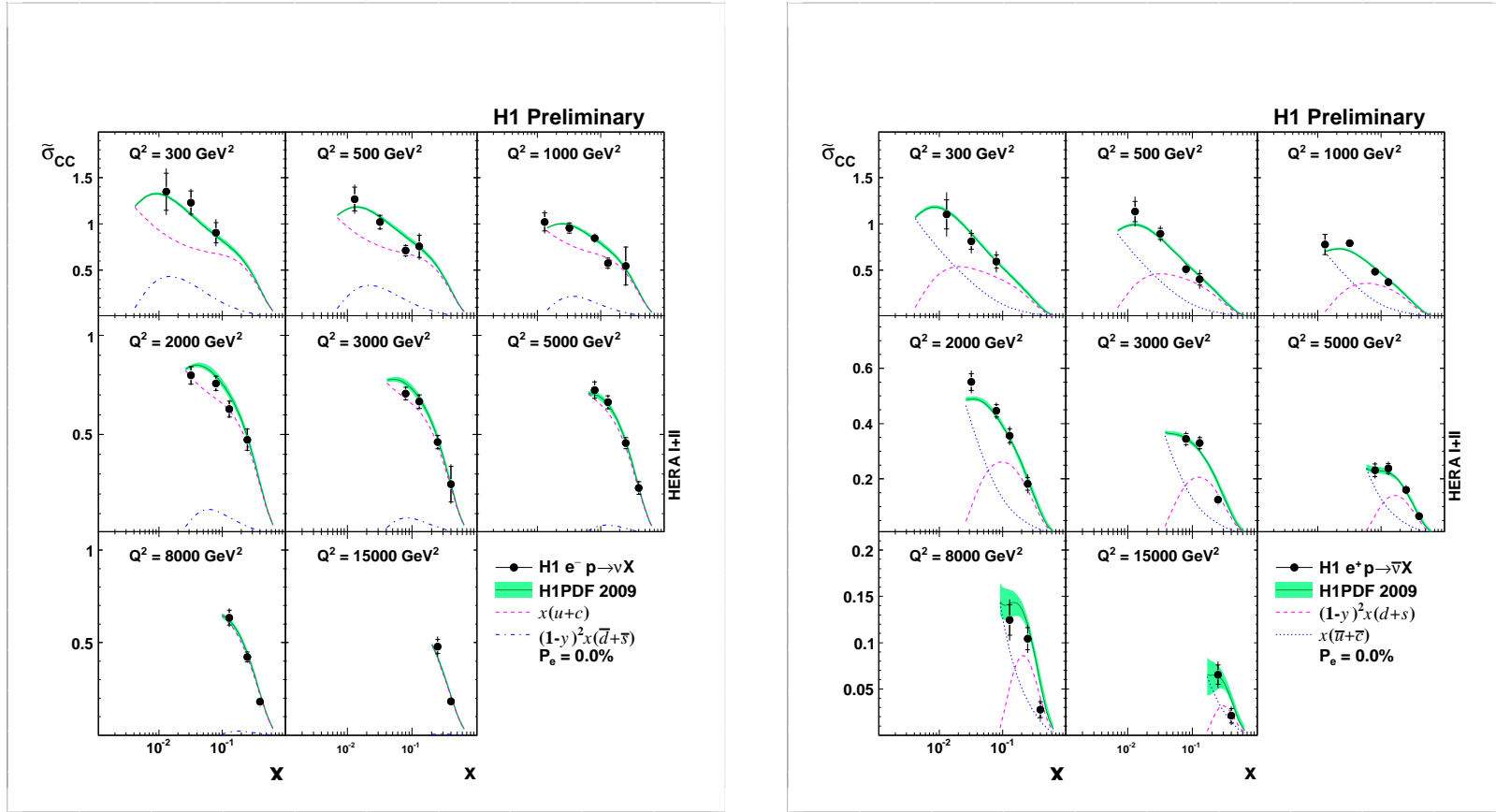
- Data:
 - Neutrino scattering data.
 - CC data from HERA.
 - xF_3 structure function from HERA.
 - Tevatron and LHC W asymmetry.
- Theory:
 - Fermion counting sum rules.
 - Lattice QCD.

xF_3 at HERA and LHeC



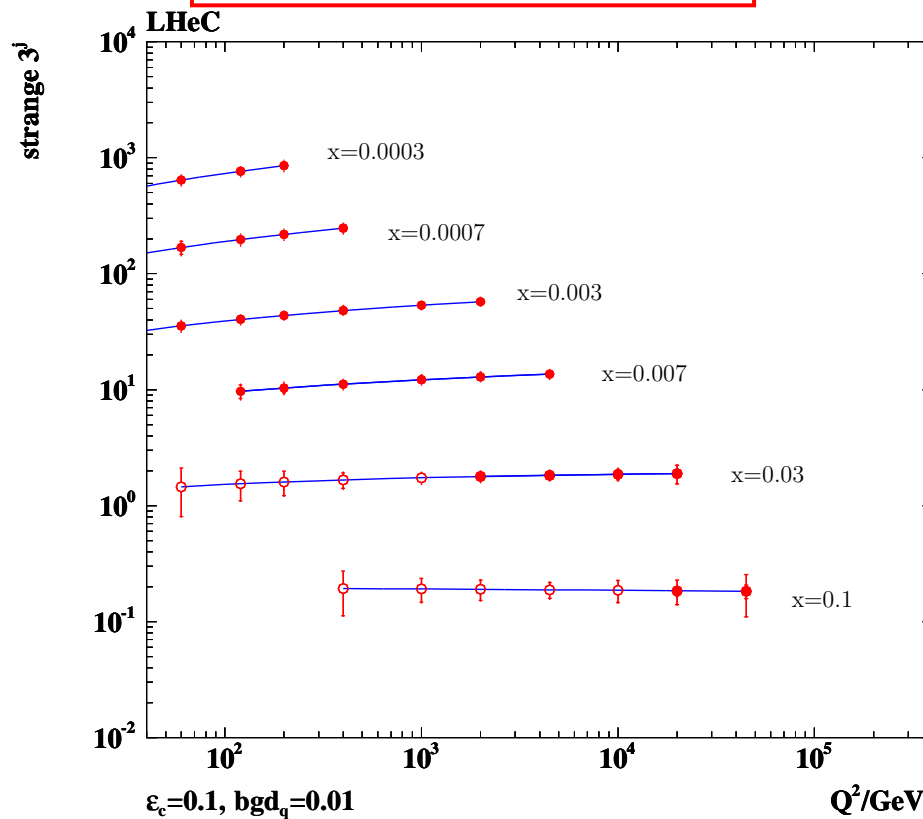
Measurement of the $x F_3$ structure function gives direct constraint on u_v and d_v quark density. It is however not sufficiently precise at HERA. LHeC could provide an extremely precise measurement down to $x = 0.001$

CC from HERA-II data



- Analysis of high Q^2 data being finalised by H1 and ZEUS.
Almost tenfold increase in $e^- p$ luminosity compared to HERA-I
- CC data constrain the decomposition of contributions from u_v, d_v and \bar{U}, \bar{D} in important for the LHC x range.

Strange density



The least known quark density at low x is the strange density. The only direct information comes from di-muon events for neutrino scattering.

$s\bar{s}$ asymmetry can be measured at the LHC by tagging the charm jet.

LHeC could provide very precise data on strange density using CC, with tagged charm.

Summary

- HERA structure function F_2 measurements provide accurate determination of the linear combination of the quark densities $4(U + \bar{U}) + (D + \bar{D})$.
- Combination of the HERA F_2^{cc} data together with theory improvements should allow to decompose contribution of heavy quarks c and b .
- Contribution of U and D quark densities can be decomposed at the LHC by comparing γ and Z exchange contributions. Data at different \sqrt{s} are very useful for that.
- Accuracy of the valence quark determination will improve with HERA-II data. Measurements of the lepton asymmetry at the LHC will have significant impact too.